

X Y Some physical properties of associative polymers

Christian Ligoure

Laboratoire Charles Coulomb

CNRS/Université Montpellier 2,

34095 Montpellier CEDEX 05, France

Contents

1	Introduction	2
2	Experimental system	3
3	Pair potential between two droplets induced by telechelic polymers [22]	4
4	Entropic phase separation in transient networks [25]	8
5	Linear viscoelastic properties	10

1 Introduction

Associating polymers are macromolecules with a part that is soluble in a selective solvent (often water), the so-called backbone or spacer to which two or more moieties that do not dissolve in this solvent, the stickers, are attached. The stickers may be randomly distributed along the backbone or may be grouped in blocks. One of the major issue of associating polymers is to convey useful rheological properties to solutions, such as increased viscosity, gelation, shear-thinning or shear-thickening. the association of such polymers in solution has been studied extensively, and many reviews can be found in the literature , see for example [1–4].

Associating polymer may form self-assembled transient networks, a class of complex materials forming spontaneously 3D networks at thermodynamical equilibrium, that can transmit transiently elastic stresses over macroscopic distances. Transient self-assembling networks are common in both natural and synthetic materials. They consist of self-assembled aggregates (nodes) that are reversibly connected by links with a finite life-time as opposed to chemical gels where junctions are permanent. These physical gels exhibit two universal and independent features : a thermodynamic first order phase separation, which occurs at low volume fraction between a dilute and concentrated solution even in the absence of any specific interaction, and a non-thermodynamic topological transition, where an infinite network spanning the entire volume of the system is formed [5].

Telechelic polymers are often used as model linkers because they are architecturally simple: they consist of a long solvophilic midblock with each end terminated by a solvophobic short chain (a sticker). The stickers incorporate into the solvophobic domains of the aggregates and can bridge them via their solvent-soluble midblock resulting in an attractive interaction between the aggregates. The nature and the morphologies of the aggregates forming the network are versatile: (i) telechelic polymers in binary solution [6] that self-assemble spontaneously into non interacting flowerlike micelles at low concentration and form three dimensional networks above a threshold concentration [7] , (ii) surfactant vesicles [8] , (iii) lyotropic lamellar phases [10] (iv) wormlike micelles [11–13], (v) spherical micelles [14], (vi) oil-in-water [15] or water-in-oil [16] microemulsion droplets.

This last system (telechelic-microemulsion mixtures) is of particular fundamental interest. Indeed, the advantage of this system is that the parameters that control the thermodynamics and structure of the physical gel can be easily identified and independently controlled: the concentration of nodes (the droplets) and the number of polymers per droplets. This is in contrast with binary mixtures of telechelics, where the number of nodes formed by the associating chain ends and the number of links cannot be controlled separately. Other advantages of this system are the spherical symmetry which allows for instance a simple structural analysis in the Fourier space from scattering experiments and the versatility of the control of the surface curvature.

On the other side, linear rheological properties are very simple and have been indeed very well described by a simple Maxwell fluid model with a single relaxation time and a single zero shear modulus. Again the elastic modulus is easily controlled by the number density of polymer bridges in the sample whereas the relaxation time can be tuned by changing the chemical length of the stickers. Finally This system exhibit a very peculiar sudden rupture mode reminiscent of a brittle fracture in solid materials [17].

So, the telechelic -micromemulsion mixtures serve as an elegant model system for a general class of transient networks of associating polymers and allow to investigate both the equilibrium, structural, flow an fracture properties of transient networks . In this lecture, we will first describe the model system, and address successively (i) the pair potential induced by two

beads reversibly linked by telechelic polymers, (ii), the phase behavior of the microemulsion-telechelics mixtures, and (iii) the linear viscoelastic properties. However, the reader interested in binary solutions of telchelic chains can refer to a series of recent papers by Sprakel *et al.* [18–20]

2 Experimental system

The telechelics-microemulsion mixture system is composed of an oil-in-water droplet microemulsion to which telechelic polymers are added. This system was previously described by Filali *et al* [15]. The o/w microemulsion involves a cationic surfactant, cetyl-pyridinium chloride CPCI, and a cosurfactant *n*-octanol. The droplets are swollen with decane and dispersed in 0.2 M NaCl brine. The droplets are spheres of radius $b = 62 \text{ \AA}$ and were found robust to variations of both the microemulsion concentration and of the amount of added polymer [15]. The volume fraction in oil droplets is denoted ϕ . The polymer chains (Poly-ethylene oxide) of molecular weight 10 kDalton are grafted at both ends with aliphatic chains of eighteen CH_2 groups. This hydrophobic end groups (stickers) anchor reversibly into the microemulsion droplets. The polymer amount is represented by the connectivity r , i.e. the average number of hydrophobic stickers per droplet. The polymers chains can either link two oil droplets (bridge configuration) or loop one a single one (loop configuration). The other possible states (free chains with no stickers adsorbed into a sphere of dangling chains with a single sticker adsorbed) are negligible. Indeed, For aqueous transient networks, the stickers consist of short chains of typically 10-25 methylene groups, with a sticking energy on the order of kT per methylene group. Therefore, the corresponding sticking energy is $\epsilon/kT \approx 10 - 25$ is large enough to neglect the fraction of dangling or free chains.

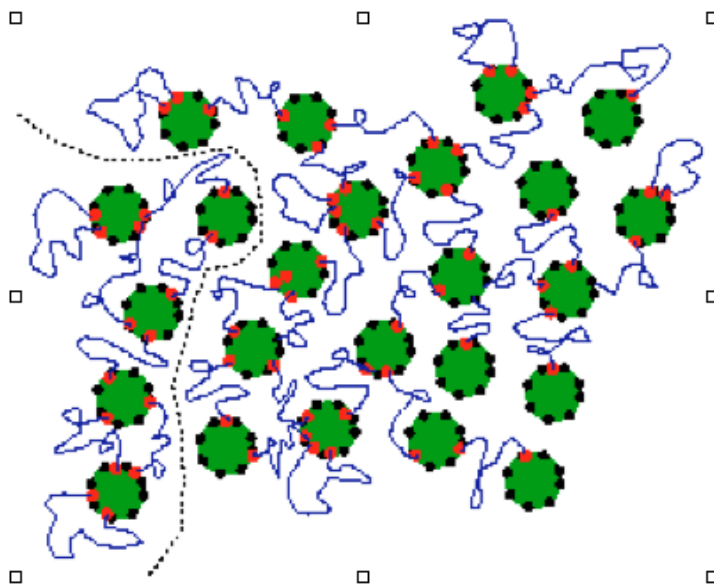


Fig. 1: Schematic of a bridged microemulsion. The telechelic polymers can either link two oil droplets or loop on a single one.

The phase diagram [21] is shown In Figure 2. For sufficiently low amount of telechelic polymers a one phase region is obtained for all volume fraction of droplets. For higher r , phase separation occurs in a wide range of droplets volume fraction. The biphasic region comprises

two isotropic and transparent phases, one being a rather stiff gel and the other being a fluid of low viscosity. In the one phase region, a sol-gel transition (this is a topological transition and not a thermodynamic transition) and defined the percolation line. A generic phase behavior is expected for mixed systems of self-assembled aggregates and polymeric crosslinkers: an entropically driven, first-order thermodynamic phase transition is predicted to occur even in the absence of any specific interactions at the mean-field level [5]. The configurational entropy of polymer junctions induces indeed an effective attraction that can result in an equilibrium between a dilute phase and a connected network.

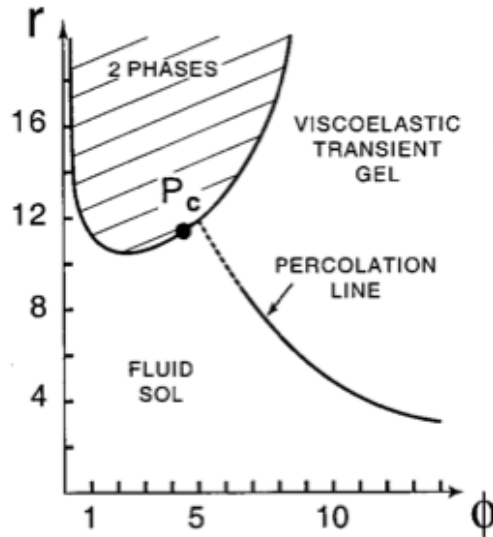


Fig. 2: Phase diagram of the connected microemulsion as a function of the droplet volume fraction ϕ and the mean number of polymer stickers per droplet r .

3 Pair potential between two droplets induced by telechelic polymers [22]

Let consider two spheres of diameter σ separated by a distance h than interact through ideal telechelic polymer chains of N monomers of size a . The polymers are in contact with a bulk reservoir of chemical potential μ . The stickers are free to diffuse onto the spheres and the sticking energy $\epsilon \gg kT$, so that the free chain configurations and the dangling chains configurations are negligible. We first consider the simpler case of two infinite walls separated by a distance h along the z axis. it consists of M sites of area a^2 which can be either occupied by a surfactant molecule or by the sticker of a telechelic polymer of polymerization index N . The statistical weight associated with all configurations of an ideal chain of N monomers located between the two impenetrable walls with its first monomer at $\mathbf{r} = (x, y, z)$ and its last one at $\mathbf{r}' = (x', y', z')$ is given by the chain propagator equation [?]:

$$\left(\frac{\partial}{\partial N} - \frac{a^2}{6} \nabla^2 \right) G_N(\mathbf{r}, \mathbf{r}') = 0 \quad (1)$$

where $G_N(\mathbf{r}, \mathbf{r}') = 0$ outside the space between the walls.

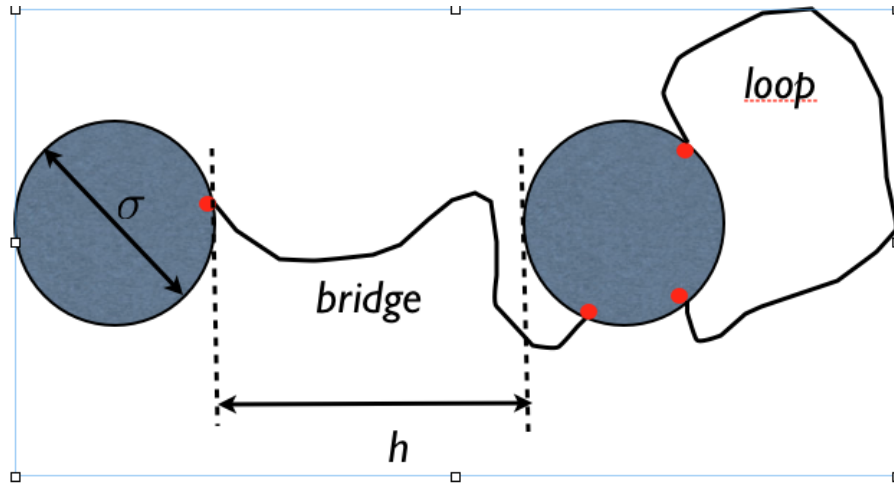


Fig. 3: Two beads interacting via a telechelic polymer

The solution of Eq.(1) is given by standard methods:

$$G_N(\mathbf{r}, \mathbf{r}') = \frac{3}{2\pi Na^2} \exp \left[-\frac{3}{2Na^2} [(x-x')^2 + (y-y')^2] \right] \times \frac{2}{h} \sum_{p=1}^{\infty} \exp \left[\frac{-\pi^2 Na^2}{6h^2} p^2 \right] \sin \frac{\pi pz}{h} \sin \frac{\pi pz'}{h} \quad (2)$$

A loop configuration is obtained by demanding that $\mathbf{r}_0 = (0, 0, a)$ and $\mathbf{r}'_0 = (x', y', a)$ and the corresponding loop partition function is:

$$z_l(h) = a \int_{-\infty}^{+\infty} dx' \int_{-\infty}^{+\infty} dy' G_N(\mathbf{r}_0, \mathbf{r}') = \frac{2a}{h} \sum_{p=1}^{\infty} e^{-\frac{\pi^2 Na^2}{6h^2} p^2} \sin^2 \frac{p\pi a}{h} \quad (3)$$

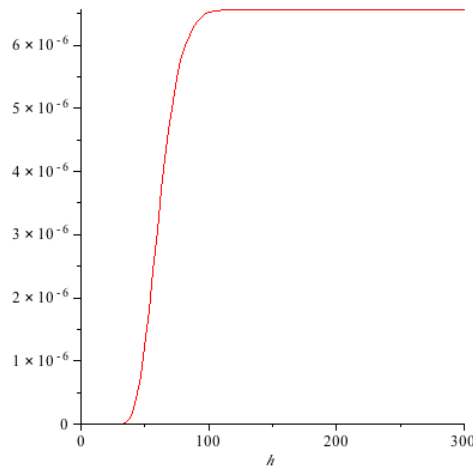


Fig. 4: Partition function of a loop (Eq. 3)

A bridge configuration is obtained by demanding that $\mathbf{r}_0 = (0, 0, a)$ and $\mathbf{r}'_0 = (x', y', h - a)$ and the corresponding bridge partition function is then:

$$z_b(h) = a \int_{-\infty}^{+\infty} dx' \int_{-\infty}^{+\infty} dy' G_N(\mathbf{r}_0, \mathbf{r}') = \frac{2a}{h} \sum_{p=1}^{\infty} (-1)^{p+1} e^{-\frac{\pi^2 N a^2}{6h^2} p^2} \sin^2 \frac{p\pi a}{h} \quad (4)$$

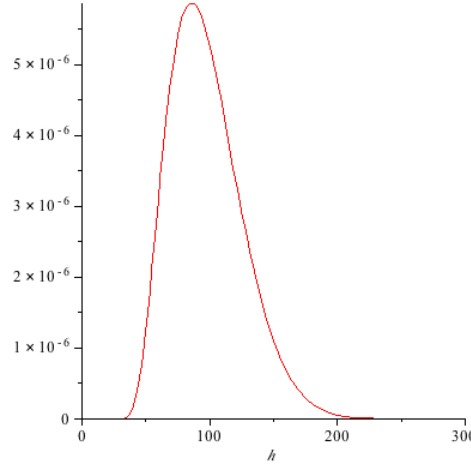


Fig. 5: Partition function of a bridge (Eq. 4)

From Eqs(3,4) one gets:

$$z_l(\infty) = \frac{3\sqrt{6}}{n^{3/2}} \quad (5)$$

$$z_b(\infty) = 0 \quad (6)$$

As expected the bridge partition function vanishes if the two wall are far apart ($h \rightarrow \infty$), whereas the loop partition function remains constant. Ideal chains by hypothesis do not interact, so, the partition function of Q ideal chains stucked on a pair of wall is:

$$Z_Q(h) = \binom{Q}{M} (z_b(h) + z_l(h))^Q \quad (7)$$

The corresponding grand partition function reads:

$$\Xi(h) = \sum_{Q=0}^M Z_Q(h) e^{\beta\mu Q} \quad (8)$$

where μ is the chemical function of a polymer chain. Note that we use the grand canonical statistical ensemble, because chains are free to exchange with the bulk reservoir. The grand potential *per unit area* is:

$$J(h) = \frac{kT}{a^2} \ln[1 + e^{\beta\mu} (z_b(h) + z_l(h))] \quad (9)$$

where z_l and z_b are given by Eqs (3,4).

The polymer-induced effective potential per unit area between the two walls is then:

$$V(h) = J(h) - J(\infty) = -\frac{kT}{a^2} \ln \frac{1 + e^{\beta\mu} z(h)}{1 + 3\sqrt{6}N^{-3/2}e^{\beta\mu}} \quad (10)$$

where:

$$z(h) = z_l(h) + z_b(h) = \frac{4a}{h} \sum_{p=0}^{\infty} e^{-\frac{\pi^2 N a^2}{6h^2} (2p+1)^2} \sin^2 \frac{(2p+1)\pi a}{h} \quad (11)$$

One has to keep in mind that the mean number of adsorbed polymer per unit area $\langle q(h) \rangle = -\partial J/\partial\mu$ is *not* a conserved quantity, that is depends on h . So, in the biphasic domain of the phase diagram, there is no reason that droplets in the dilute phase bear the same mean number of polymers than droplets in the gel phase.

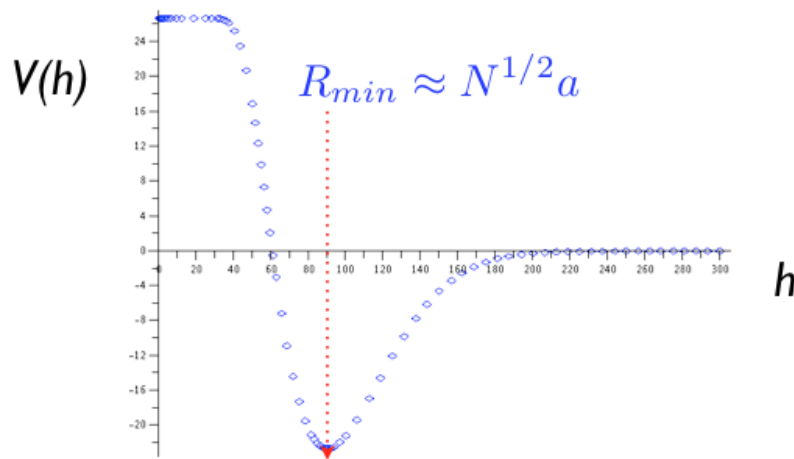


Fig. 6: Polymer induced effective potential per unit area between two walls

The effective pair potential induced by telechelic polymers $V(h)$ is plotted in Fig.(6). It exhibits an attractive minimum for a distance between the walls on the order of the end to end distance of a polymer chain $R = aN^{1/2}$; for this distance, the fraction of bridges is maximal. At larger distances, there is an entropic penalty for the bridge configurations because bridges must be stretched. At shorter distance the entropic cost of polymer confinement (for both loops and bridges configurations) induces an effective repulsion between the walls.

To extend these results to curved surfaces, we use the Derjaguin approximation despite the fact that the curvature of the droplets are of the same order of magnitude than the size of polymer chain. The Derjaguin approximation [23] is a powerful approximation widely use in colloidal science which gives the force between two spheres in terms of the energy per unit area of two flat surfaces at the same separation it is applicable to any type of force law, whether attractive, repulsive or oscillatory, so long as the range of the interaction and the separation is much less than the radii of the spheres . Finally on obtains the contribution $V_p(h)$ of the polymer to the interaction potential between the droplets of diameter σ at distance h from Eqs.(10,11):

$$V_p(h) = \frac{\pi\sigma}{2} \int_{\infty}^h V(h') dh' \quad (12)$$

The potential V_p is plotted in Figure(7)

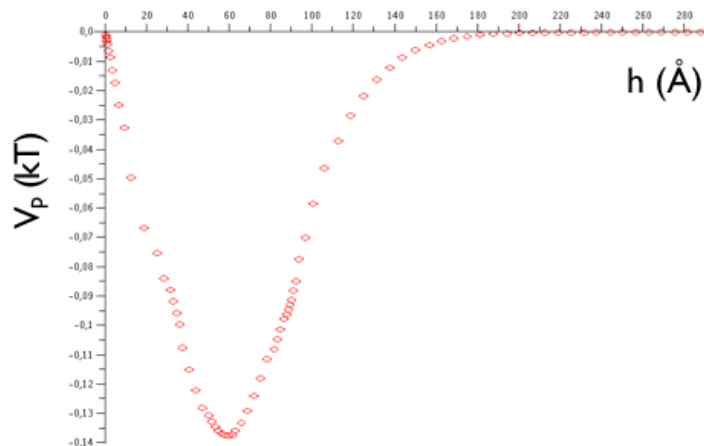


Fig. 7: Polymer induced effective potential per unit area between two spheres (??)

The attractive minimum for a distance between spheres on the order of the polymer end to end distance is still present. However the repulsion at short distances disappears. This is a consequence of the fact that, even at close contact, a bridge or a loop can exist because the stickers freely slide onto the spheres as shown by Monte Carlo simulations [24]; For real chains, where the potential is non additive with the mean number of polymer/per bead, the simulations show the repulsion due to the entropic confinement of the polymer chains. The effective potential V_p has been tested to fit the small angle neutron scattering data for the structure factor of the experimental system [22]: the agreement is qualitative; however, the potential underestimates the repulsion between the spheres, due to the sliding effect, which becomes less and less important for the $N > 2$ bodies contributions to the potential between spheres.

4 Entropic phase separation in transient networks [25]

A simple mean-field theory has been developed by Zilman *et al* [25] to explain the experimental phase diagram shown in Fig.2. It predicts how the polymer properties control the phase behavior. The predicted phase separation has a *purely entropic origin*: there are no energetic interactions among the polymers or droplets. The phase separation occurs because the loss of the translational entropy of the droplets is overcompensated by the high configurational entropy of the polymer connections in the dense network.

A total of N_p polymers and \mathcal{N} beads are distributed in space so that a polymer either connects two beads or loops on a single bead. The total free energy of the systems which is athermal amounts to the configurational entropy. The first term is the translation entropy of mixing of a dispersion of hard spheres given in lattice representation by:

$$S_0 = -k[\phi \ln \phi + (1 - \phi) \ln(1 - \phi)] \quad (13)$$

where $S_0(\phi)$ is the entropy per site on the lattice and ϕ is the volume fraction of the beads. The second contribution is the configurational entropy of distributing the polymers among the beads.

For a single polymer there are $q_l \mathcal{N}$ available looped states where q_l is the number of positions

available to a sticker of size a at the surface of a drop: $q_l \simeq \sigma^2/a^2$ (σ is the diameter of a bead). The free energy cost ϵ_l (in kT units) of a looped polymer measures the entropic cost of both ends being confined to the same droplet. In a simple approximation, the number of configurations available to a polymer with radius R_G , and with both ends constrained to a volume v , that is small relative to the total volume is proportional to $(v/R_G^3) \simeq \sigma^2 l/R_G^3$ where l is the length of the hydrophobic sticker. Therefore $e^{-\epsilon_l} \simeq (\sigma^2 l/R_G^3)$ for $\sigma < 2R_G$ and saturates to unity for $\sigma > 2R_G$.

We calculate now the mean number of beads connected by a polymer. For a bead located at the origin O , the mean number of droplets at a distance $[R, R + dR]$ is $\frac{4\pi R^2 dR \phi}{\pi \sigma^3/6}$. This gives the number of pair droplets at a distance $[R, R + dR]$ ($R > \sigma$)

$$\frac{\mathcal{N}}{2} \frac{4\pi R^2 dR \phi}{\pi \sigma^3/6} = q(R) dR \quad (14)$$

A bridge connecting two beads at distance R has stretching energy on the order of $E_R = \frac{3}{2} kT R^2 / (N a^2)$.

The partition function of a single chain is:

$$Z_1 = q_l \mathcal{N} e^{-\epsilon_l} + \int_{\sigma/2}^{\infty} q(R) e^{-E(R)/(kT)} dR = q_l \mathcal{N} e^{-\epsilon_l} + q \phi \mathcal{N} \quad (15)$$

with

$$q = \int_{\sigma/2}^{\infty} \frac{24R^2}{\sigma^3} \exp\left(-\frac{3}{2} \frac{R^2}{N a^2}\right) dR \quad (16)$$

The partition function of N_p chains which are undistinguishable and independent is:

$$Z_p = \frac{1}{N_p!} Z_1^{N_p} = \frac{(q_l \mathcal{N} e^{-\epsilon_l} + q \phi \mathcal{N})^{N_p}}{N_p!} \quad (17)$$

The free energy per lattice site of the system is $f = -kT/V (\ln Z_p - T S_0(\phi))$. From Eqs.(13, 17) with $c = N_p/V$ and $\phi = \mathcal{N}/V$ one gets:

$$\frac{f(\phi, c)}{kT} = \phi \ln \phi + (1 - \phi) \ln(1 - \phi) + c(\ln c - 1) - c \ln(q \phi^2 + \phi q_l e^{-\epsilon_l}) \quad (18)$$

The first and second terms in Eq.(18) corresponds to the translational entropy of the droplets; the third term corresponds the translational entropy of the polymers, and the last term describes the effective interaction between the droplets and the polymers.

The mixed system is stable if $f(\phi, c)$ is a convex function, i.e $\delta^2 f = f_{\phi\phi} \delta\phi^2 + 2f_{\phi c} \delta\phi \delta c + f_{cc} \delta c^2$ should be a positive bilinear form. So, the matrix

$$\mathbf{S} = \begin{pmatrix} f_{\phi\phi} & f_{\phi c} \\ f_{\phi c} & f_{cc} \end{pmatrix}$$

must have two positive eigenvalues. Simple algebraic manipulations show that f_{cc} is positive, so the condition of stability reduces to $\det \mathbf{S} > 0$, i.e.:

$$2 \frac{c}{\phi} < \frac{\phi + (q_l/q) e^{-\epsilon_l}}{\phi(1 - \phi)} \quad (19)$$

The mean number of stickers per bead is $\bar{r} = 2c/\phi$, so the spinodal is defined by

$$\bar{r} = r_s = \frac{\phi + (q_l/q)e^{-\epsilon_l}}{\phi(1 - \phi)} \quad (20)$$

Eq.(20) defines the spinodal line in the plane (ϕ, r) , i.e., if $r > r_s$, the system is thermodynamically unstable and phase separates into a system of dense droplets that are highly connected by polymers, that coexists with a dilute system of almost disconnected droplets, decorated with polymer loops. The latter observation stems from the fact that the average fraction of the looped polymers $\bar{\lambda}$ is given by:

$$\bar{\lambda} = \frac{-\partial \ln Z_1}{\partial \epsilon_l} = \frac{(q_l/q) \exp(-\epsilon_l)}{(q_l/q) \exp(-\epsilon_l) + \phi} \quad (21)$$

In the dilute phase $\phi \rightarrow 0$ and $\bar{\lambda} \rightarrow 1$

In the coexistence phase domain, the equality of the polymer chemical potentials $\mu_c = \partial f / \partial c$ in the two coexisting phases implies that:

$$r = m \left(\phi + \frac{q_l}{q} e^{-\epsilon_l} \right) \quad (22)$$

where m is a constant defined by $m = \frac{2e^{\mu_c}}{q}$. It follows that the coexisting phases lie along the lines given by Eq.(22), which are *not* horizontal in the (ϕ, r) plane.

Intersection points of the coexisting lines Eq(22) and the spinodal Eq.(20) are the solutions of the equation $\phi^2 - \phi + m = 0$. For $m < 4$ there is no solution, and so no phase coexistence. For $m = 4$, there is a single solution ($\phi = 0.5; r = r_c = 2 + 2\frac{q_l}{q}e^{-\epsilon_l}$) which defines the critical point that is *not* the minimum of the spinodal. For $m > 4$ there are two solutions (be careful that these solutions do not define the binodal). These simple analytical results reproduce qualitatively well the phase behavior of the experimental system and are summarized in Figure 8. Computer simulations of the same system [26] verify the predictions of the analytical model. Because of its entropic nature, the phase separation is extremely robust and is independent of the detailed assumptions about the polymer and/or the nodes properties. For instance it is also predicted using a self consistent field theory for binary solutions of telechelic chains [19] in agreement with experimental results [27], [28]. The same type of phase separation has been also observed with entangled solutions of wormlike micelles bridged by telechelic polymers [11].

5 Linear viscoelastic properties

The gel phase of the bridged microemulsion behaves as a Maxwell, fluid, that is the simplest viscoelastic behavior: the material can be characterized by a single plateau shear modulus μ_0 and a single relaxation time τ . The constitutive differential scalar equation of a Maxwell fluid is obtained from the spring and dashpot representation of a Maxwell element (Fig. 9).

$$\sigma + \tau \frac{d\sigma}{dt} = \eta \frac{d\gamma}{dt} \quad (23)$$

where σ is the shear stress, γ is the shear strain and $\eta = \mu_0\tau$ is the viscosity of the Maxwell fluid.

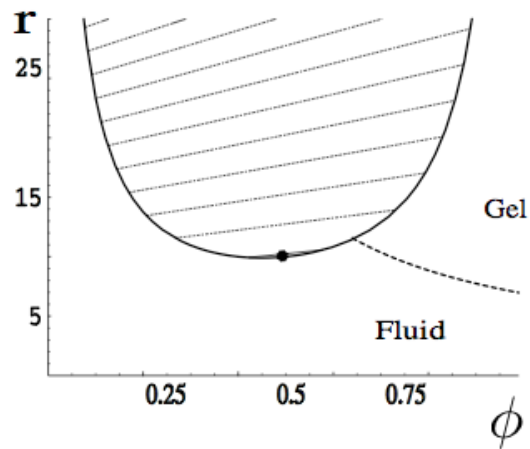


Fig. 8: Phase diagram [25] of drops connected with polymers. The thick line is the spinodal line of the phase separation for $q_1 e^{-c_1}/q = 2$. Above this line the system becomes thermodynamically unstable. The critical point is at $\phi = 0.5$ and is shown as a black dot. Note that the critical point is not at the minimum of the spinodal. The tie lines are shown as dotted lines in the phase separation region. Note that they are not horizontal. The dashed line shows the percolation threshold calculated for an fcc lattice with $q = 16$. Below the percolation line, the system is in the fluid state, while above it a connected gel is formed

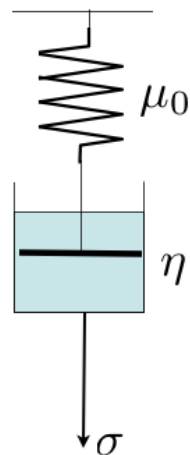


Fig. 9: Spring and dashpot representation of a Maxwell element

When a Maxwell fluid is submitted to an oscillatory stress at frequency ω characterized by its complex form $\underline{\sigma} = \sigma_0 \exp i\omega t$ the material response given by the complex strain $\underline{\gamma}$ is of the form $\underline{\sigma} = \underline{\mu}(\omega)\underline{\gamma}$.

$Re(\underline{\mu}(\omega)) = \mu'(\omega)$ defines the storage modulus of the material and $Im(\underline{\mu}(\omega)) = \mu''(\omega)$ is the loss modulus. From Eq. 23, one gets the storage and loss moduli for a Maxwell fluid:

$$\mu'(\omega) = \mu_0 \frac{(\tau\omega)^2}{1 + (\tau\omega)^2} \quad (24)$$

$$\mu''(\omega) = \mu_0 \frac{\tau\omega}{1 + (\tau\omega)^2} \quad (25)$$

At low frequency ($\omega\tau \ll 1$), the modulus is purely imaginary ($\mu = i\omega\mu_0\tau$) and the material behaves as a liquid of viscosity $\eta = \mu_0\tau$. At high frequency ($\omega\tau \gg 1$) we are dealing with an elastic solid with an elastic modulus $\mu \approx \mu_0$.

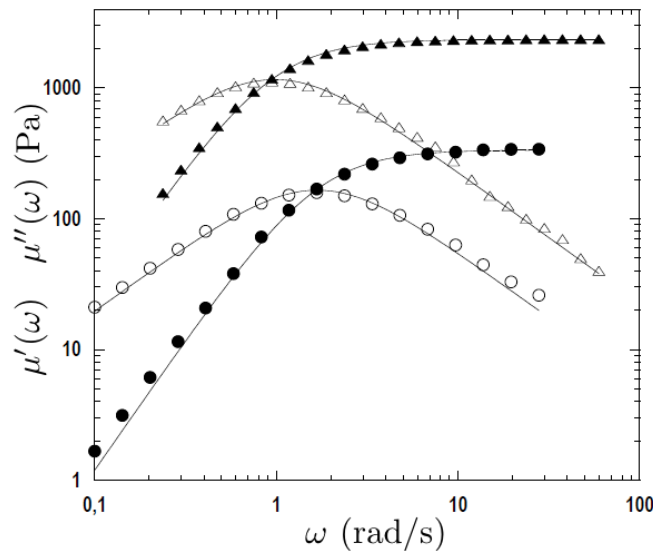


Fig. 10: Frequency sweep experiments. Storage modulus, μ' (closed symbols) and loss modulus, μ'' (opened symbols) as a function of the frequency ω for the fluids [$r = 6, \phi = 10\%$] (circles) and [$r = 12, \phi = 10\%$] (triangles). Solid lines correspond to fits by a Maxwell mode (Eqs. 24, 25) which give the elastic shear modulus and the relaxation time of each fluid.

Figure 10 show that the Maxwell behavior is almost perfect for the telechelics-microemulsion mixtures. The shear modulus and the relaxation time are respectively equal to 330 Pa and 0.59 s for [$r = 6, \phi = 10\%$], 2400 Pa and 2 s for [$r = 12, \phi = 10\%$] [29].

The origin of the Maxwell behavior is explained by the transient network theory [30]. We summarize here the main results. At high frequency, where we can neglect the transient nature of the network the gel is a a polymer network. The simplest model to describe the elastic properties of a permanent polymer network like a rubber is the affine network model which is described in textbooks (see for instance Ref. [32]). The elasticity arises primarily from the changes in entropy of the network strands when the network is macroscopically deformed. So the shear modulus is:

$$\mu_0 = n_b kT \quad (26)$$

where $n_b \propto \frac{r}{2}\phi$ is the number density of polymer bridges. The stress relaxation arises from the finite residence time τ_R of a sticker in a given droplet. Since the escape of a given sticker from a droplet is presumably a thermally activated process, we expect τ_R and therefore $\tau \propto \tau_R$ to exhibit an Arrhenius dependance versus the temperature:

$$\tau = \tau_0 \exp(E_s/kT) \quad (27)$$

where τ_0 is some inverse frequency of attempts and the activation energy E_s is the reversible work of extraction of the sticker from the hydrophobic core into the free water. The activation energy is itself proportional to the number of methyl groups n_{CH_2} in a sticker $E \simeq 1.2kTn_{CH_2}$. The longer are the stickers of the telechelic chains, the longer is the relaxation time of the network.

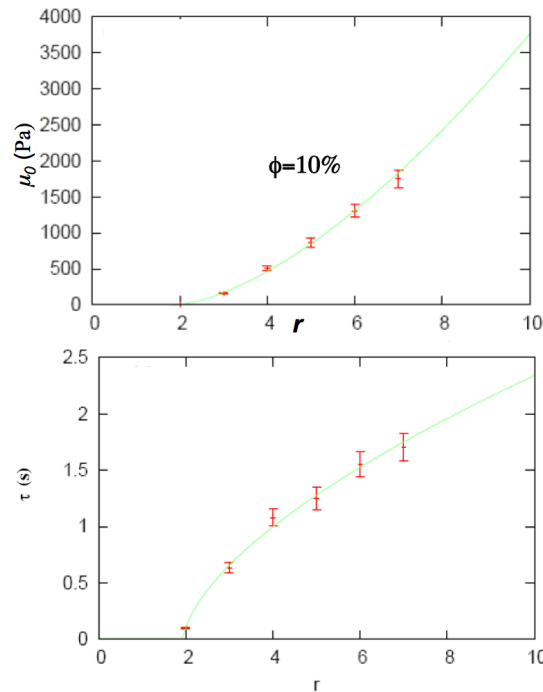


Fig. 11: Evolution of the shear modulus μ_0 and the relaxation time τ near the percolation threshold (Note that in these experiments the polymer chains have a molecular weight of 35kDa). The lines are fits with the expressions $\mu_0(\text{Pa}) = 389(r - 1.9)^{1.55}$ and $\tau(\text{s}) = 0.6(r - 1.9)^{0.6}$

Eqs (26,27) do not describe properly the viscoelastic behavior near the percolation line as shown in Figure 11. For a given droplet concentrations both the elastic plateau modulus and the relaxation time exhibit a power law dependance with the apparent connectivity r on the form $\mu_0(r) = A(r - r_p)^\alpha$ and $\tau = B(r - r_p)^\beta$, where r_p defines the percolation point of the network for a given ϕ [33]. In principle, in percolation situations, the singular power law dominates the evolution of a given quantity only close to the threshold. Far above, the mean field behavior is

usually recovered. In contrast, in this system, the fits happen to be surprisingly good even far above $r_p(\phi)$ a feature that is not understood.

μ_0 characterizes the immediate elastic response of the network to a sudden deformation, before any relaxation due to the finite lifetime of a link. It is natural in this picture that it vanishes below a finite value r_p of the connectivity parameter: below r_p , there is no cross-linked infinite path, connecting continuously the cone and the plate of the rheometer and capable of sustaining the transient elastic torque. Since by definition μ_0 does not involve any feature related to relaxations, its evolution can be compared to theoretical predictions derived at true sol-gel transitions. The exponent calculated for the elastic modulus is 1.7 above the gel point [34] close to the value measured in this system. The terminal relaxation time τ is related to the residence time of a sticker in a droplet. In the usual interpretation of the stress relaxation in transient networks [30, 31] the spatial distribution of the nodes is assumed to be affinely deformed by the step strain and the length distribution of the links is thus shifted accordingly. The transient off equilibrium length distribution is at the origin of the measured stress. From time to time stretched links disengage due to the finite residence time of their stickers and reconnect with the equilibrium length distribution: they forget the initially imposed strain and no more contribute to the stress. In this picture the stress at time t is a simple measure of the number of links that still reminds the initial strain after time t , and we would expect τ to be simply identical to the residence time. The measurements do not support this expectation: τ sensitively depends on the average degree of connectivity r and vanishes at r_p , whereas the residence time is completely determined by the adsorption energy of a sticker in a droplet. It should not depend on nonlocal features such as the degree of connectivity of the network. To understand the discrepancy, we note that the above affine picture is a mean field description which assumes that the imposed strain distributes homogeneously within the network. Such homogeneity certainly breaks when approaching the percolation point. Close to the threshold, the infinite connected cluster consists of more densely cross-linked subclusters connected to each other by weaker parts where the links are less dense. Breaking a small number of links only, in a weak part, will suddenly release the stress within the whole adjacent dense subclusters. In this non-mean-field picture, we expect τ to be shorter than the residence time and indeed to vanish at the percolation as observed in the experiments.

References

- [1] R.G. Larson, *The structure and rheology of complex fluids* (Oxford University press, Oxford, 1999)
- [2] M.A. Winnik and A. Yekta *Curr. Opin. Colloid Interface Sci.* **2**, 424 (1997).
- [3] JF. Berret, D. Calvet, A. Collet, M. Viguier *Curr. Opin. Colloid Interface Sci.* **8**, 296 (2003).
- [4] C. Chassenieux, T. Nicolai, L. Benyahia *Curr. Opin. Colloid Interface Sci.* **doi: 10.1016/j.cocis.2010.07.007**, (2010).
- [5] Zilman, A.G., Safran S. A., *Europhys. Lett.* **63**, 139 (2003).
- [6] Semenov, A.N., J.F. Joanny, and A.R. Khokhlov *Macromolecules* **28**, 1066 (1995).
- [7] Annable, T., R. Buscall, R. Ettelaie, and D. Whittlestone, *J. Rheology* **37**, 695 (1993).
- [8] Lee J. H., Gustin J. P., Chen T. H., Payne G. F. and Raghavan S. R. *Langmuir* 2005 **21**, 26 (2005).
- [9] Zhu, C., J.H. Lee, S.R. Raghavan, and G.F. Payne, *Langmuir* **22**, 2951 (2006).
- [10] Warriner H. E., Davidson P., Slack N. L., Schellhorn M., Eiselt P., Idziak S. H. J., Schmidt H. W., Safinya C. *J. Chem. Phys.* **107**, 3707 (1997).
- [11] Ramos L., Ligoure C. *Macromolecules* **40**, 1248 (2007).
- [12] Lodge T. P., Taribagil R., Yoshida T., Hillmyer M. A. *Macromolecules* **40**, 4728 (2007).
- [13] Nakaya-Yaegashi K., Ramos L., Tabuteau H., Ligoure C. *J. Rheol.* **52**, 359 (1993).
- [14] Appell J., Porte G., Rawiso M. *Langmuir* **14**, 4409 (1998).
- [15] M. Filali, R. Aznar, M. Svenson, G. Porte and J. Appell, *J. Phys. Chem. B* **103**, 7293 (1999).
- [16] Bagger-Jørgensen H., Coppola L., Thuresson K., Olsson U. and Mortensen K. *Langmuir* **13**, 4204 (1997).
- [17] Tabuteau, H., Mora, S., Porte G., Abkarian M. and Ligoure C. *Phys. Rev. Lett.* **102**, 155501 (2009).
- [18] Sprakel J, Besseling NAM, Leermakers FAM, et al *J. Phys. Chem. B* **111**, 2903 (2007).
- [19] Sprakel J, Besseling NAM, Leermakers FAM, et al *EPJE* **25**, 163 (2008).
- [20] Sprakel J, Spruijt E, van der Gucht J, et al. *Soft Matter* **5**, 4748 (2009).
- [21] Filali, M., Ouazzani M. J., Michel E., Aznar, G. Porte and J. Appell, *J. Phys. Chem. B* **105**, 10528 (2001).

- [22] G. Porte, , C. Ligoure , J Appell R. Aznar, *J.Stat. Mechanics : theory and experiments* **P05005**, (2006).
bibitemdeGennes1969 de Gennes P. G. *Rep. Prog. Phys.* **32**, 187 (1969).
- [23] B. V. Derjaguin, *Kolloid. Zeits.* **69**, 155 (1934).
- [24] Testard V., Oberdisse J. and Ligoure C. *Macromolecules* **41**, 7219 (2008).
- [25] Zilman A., Kieffer J., Molino F., Porte G. And Safran S. A. *Phys. Rev. Lett* **91**, 015901 (2003).
- [26] Hurtado, P., Berthier L. and Kob W. *Phys. Rev. Lett.* **98**, 135503 (2007).
- [27] Pham, Q. T., Russel W. B., Thibeault J. C., Lau W. *Macromolecules* **32**, 2996 (1999).
- [28] François J., Beaudoin E., Borisov O. *Langmuir* **19**, 1011 (2003).
- [29] Tabuteau H., Mora S., Ciccotti M. and Ligoure C. *submitted to Soft Matter* , ().
- [30] Green M. S. and Tobolsky A. V. *J. Chem. Phys.* **14**, 80 (1946).
- [31] Tanaka F; and Edwards S. F. *Macromolecules* **25**, 1516 (1992).
- [32] Rubinstein M. and Colby R. H. *Polymer Physics* (Oxford University Press, New-York, 2003)
- [33] Michel E., Filali M., Aznar R., Porte G. and AppellJ. *Langmuir* **16**, 8702 (2000).
- [34] Stauffer D. *Introduction to percolation theory* (Taylor Francis, London, 1985)